# Classification of Wavelet-denoised Musical Tone Stimulated EEG Signals using Artificial Neural Networks

Roy Francis Navea
Electronics and Communications Engineering Department
De La Salle University
Manila, Philippines
roy.navea@dlsu.edu.ph

Elmer Dadios
Manufacturing Engineering and Management Department
De La Salle University
Manila, Philippines
elmer.dadios@dlsu.edu.ph

***Abstract*—Electroencephalogram (EEG) signals contains information which may be of interest for a certain purpose. However, this information may be clouded by noise. The necessity of extracting this information using filtering and feature extraction techniques is of great importance. In this study, the wavelet de-noising was implemented instead of the usual frequency filter methods. Daubechies (usually denoted by 'db') wavelets ('db1' to 'db10') were utilized to determine if wavelet-based de-noising is effective in preparing musical tone stimulated EEG signals for feature extraction leading to classification. The selection of wavelet is based on signal-to-noise ratio (SNR), peak signal-to-noise ratio (PSNR), mean square error (MSE) and correlation coefficient (R). Twelve features were used and fed into an artificial neural network for classification. Results show that among the ten wavelets used, 'db8', 'db9' and 'db10' were found to be useful having satisfied the selection criteria. The EEG signals were divided into 5 segments: Baseline, secondary baseline, C, F and G. It was found out that each segment can be classified using different wavelets with correct classification accuracy ranging from 80% to around 92%.**

***Keywords—Electroencephalogram; wavelet de-noising; feature extraction; Artificial Neural Networks***

## I. INTRODUCTION

A new sound can capture our attention. However, this occurrence is also an indication that a sound either disappears or overlaps with another [1]. Attention is a complex cognitive function that deals with the selection process of both external and internal events. Music can be both an external and an internal event wherein as for this study, external musical tones were used to stimulate the brain to give a significant response which is measured in the electroencephalogram or EEG.

The EEG is a record of the electrical activities of the brain which is commonly measured using non-invasive electrodes that usually come with a headset or in the form of a neuroheadset placed on the scalp. EEG signals are widely used in clinical research [2] [3] [4], brain-computer interface (BCI) studies [5] [6] as well as music-related EEG data gathering and analysis [7]–[13].

The complexity of EEG signals post challenges in the manner of how to process them in order to extract useful information. A common approach is to use high-order frequency filter based methods. Artefacts and noise removal using selective frequency filtering methods suffer from substantial loss of EEG data. Hence, wavelet-based filtering is a good option due to its capability to deal with both time and frequency maps of the given signal simultaneously [14]. There are more than a hundred wavelets available according to [15] which are generally defined by their mother wavelets: Daubechies, Coiflets, Biorthogonal, Reverse Biorthogonal, Discrete Meyer and Symlets. Each has their own forms and characteristics.

Feature extraction and selection techniques are used to determine the significant characteristics of a certain signal segment of interest. Both time-domain and frequency-domain features including statistical characteristics [16] [17] [18] [19] [20] can be used for as long as these features and characteristics can possibly differentiate one segment from another.

Artificial neural networks (ANN) are very useful in creating classification models for a number of non-linear systems [21] [22] [23]. In this study, ANN were utilized to provide a robust classification model for wavelet - de-noised musical tone stimulated EEG signals.

## II. METHODS

### A. Audio Stimulus and Experimental Data

The audio stimulus is composed of 3 musical tones, C, F and G, which are located at the 4th octave of a standard piano keyboard. The musical piece [24] [25] used is shown in Fig. 1.

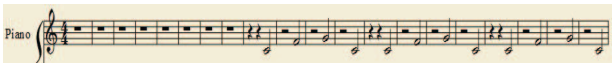


Fig. 1. Audio Stimulus Piece

978-1-5090-2597-8/16/$31.00 ©2016 IEEE

The piece is composed of rests and notes. Rests are periods of silence while the notes are the tones. The long series of rests before the first tone establishes the baseline (baseline1) while the rests that come immediately after a note is the secondary baseline (s-baseline). For synchronization purposes, a timing table [24] [25], as shown in Table I, was used to easily determine where in time a tone was played and stimulated the brain. No delays were assumed.

The timing table is the breakdown of the audio stimulus in Fig. 1 in relation to the EEG signal obtained in terms of the stimuli, time stamp, period, number of samples and sample series. The stimuli were named baseline1, s-baseline, C, F and G. The audio was played for 3 minutes and 48 seconds. Baseline 1 has the longest period with 180 seconds. S-baseline and the notes have a period of 2 seconds for each occurrence. The EEG signal was sampled at 128 samples per second. Baseline 1 has the largest number of samples with 23040. S-baseline and the notes have 256 samples each. The total number of samples is 29184 corresponding to the total period of the audio stimulus. Each stimulus was mapped in the sample series for segmentation purposes.

TABLE I. AUDIO STIMULUS TIMING TABLE

| Stimuli | baseline1 | s-baseline | C | s-baseline | F | s-baseline | G |
|---|---|---|---|---|---|---|---|
| Time Stamp | 0 - 3:00 | 3:01-3:02 | 3:03-3:04 | 3:05-3:06 | 3:07-3:08 | 3:09-3:10 | 3:11-3:12 |
| Period | 180 sec | 2sec | 2sec | 2sec | 2sec | 2sec | 2sec |
| No. of Samples | 23040 | 256 | 256 | 256 | 256 | 256 | 256 |
| Sample Series | 1-23040 | 23041-23296 | 23297-23552 | 23553-23808 | 23809-24064 | 24065-24320 | 24321-24576 |

| Stimuli | s-baseline | C | s-baseline | C | s-baseline | F | s-baseline |
|---|---|---|---|---|---|---|---|
| Time Stamp | 3:13-3:14 | 3:15-3:16 | 3:17-3:18 | 3:19-3:20 | 3:21-3:22 | 3:23-3:24 | 3:25-3:26 |
| Period | 2sec | 2sec | 2sec | 2sec | 2sec | 2sec | 2sec |
| No. of Samples | 256 | 256 | 256 | 256 | 256 | 256 | 256 |
| Sample Series | 24577-24832 | 24833-25088 | 25089-25344 | 25345-25600 | 25601-25856 | 25857-26112 | 26113-26368 |

| Stimuli | G | s-baseline | C | s-baseline | C | s-baseline | F |
|---|---|---|---|---|---|---|---|
| Time Stamp | 3:27-3:28 | 3:29-3:30 | 3:31-3:32 | 3:33-3:34 | 3:35-3:36 | 3:37-3:38 | 3:39-3:40 |
| Period | 2sec | 2sec | 2sec | 2sec | 2sec | 2sec | 2sec |
| No. of Samples | 256 | 256 | 256 | 256 | 256 | 256 | 256 |
| Sample Series | 26369-26624 | 26625-26880 | 26881-27136 | 27137-27392 | 27393-27648 | 27649-27904 | 27905-28160 |

| Stimuli | s-baseline | G | s-baseline | C |
|---|---|---|---|---|
| Time Stamp | 3:41-3:42 | 3:43-3:44 | 3:45-3:46 | 3:47-3:48 |
| Period | 2sec | 2sec | 2sec | 2sec |
| No. of Samples | 256 | 256 | 256 | 256 |
| Sample Series | 28161-28416 | 28417-28672 | 28673-28928 | 28929-29184 |

The data used were taken from 33 undergraduate students with age typically ranging from 18 to 21. As in [25], the respondents were seated one at a time in an acoustically prepared room. The lighting is dim and they were asked to close their eyes to minimize eye-related artefacts. An ear phone was used for optimal audio reception. A 14-channel Emotiv EPOC neuroheadset was used and its performance was carefully monitored through its graphical user interface.

## B. Preprocessing

The raw EEG signals were grouped using the sum of channels [26]. They were filtered between 8 Hz to 30 Hz to cover both alpha and beta bands. The filtered EEG signals were normalized [27] and segmented [28] according to Baseline (BL), s-baseline or secondary baseline (s-BL), C, F and G (as shown in Fig. 2) with respect to the timing table as shown in Table I.

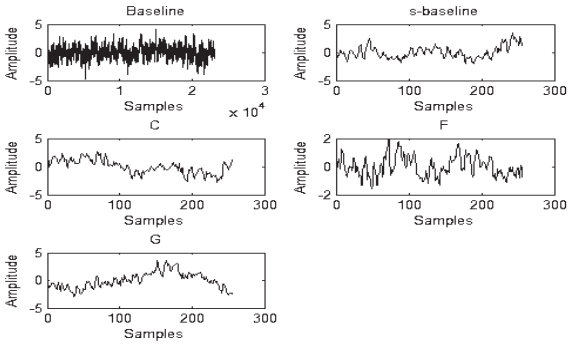


Fig. 2. Sample EEG for the segments: Baseline, s-baseline, C, F, and G

## C. Wavelet De-noising

The commonly used wavelets for de-noising are the orthogonal Meyer wavelets and the Daubechies, with a short name 'db', wavelets [14]. In [29] [30], 'db2', 'db3', 'db4', 'db6', 'db14' and 'db16' were used. However, the nature of the EEG signals used is different.

For an initial study dealing with musical tone stimulated EEG signals, the Daubechies wavelets, 'db1' to 'db10', were used. The 'db1' wavelet is also known as the Haar wavelet. Its form can be described as a simple square wave. The waveforms of 'db2' to 'db10' are shown in Fig. 3.

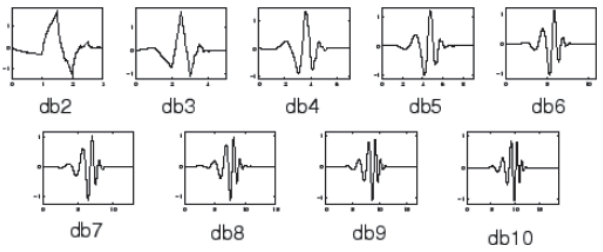


Fig. 3. Daubechies Wavelets (db2 – db10) [31]

De-noising using linear filters is not a suitable choice for functions with discontinuities due its natural process of forbidding it to estimate discontinuities efficiently. In contrast, wavelet-based de-noising using thresholding allows an adaptive representation of signal discontinuities. There are several thresholding techniques available but in this study, the threshold selection rule is based on sqrt (2*log(length(x(n)))) which is commonly known as "sqtwolog". This thresholding uses a fixed-form threshold which yields minimax performance multiplied by a small factor which is proportional to the logarithmic value of the length of x(n) or the input signal.

In order to determine which wavelet has the best de-noising effect, the signal-to-noise ratio (SNR), peak signal-to-noise ratio (PSNR), mean square error (MSE) and the correlation coefficient (R) were calculated using (1) - (4), respectively. The original EEG signal is $x(n)$ while the de-noised EEG signal is $x_d(n)$. Maximum values for SNR, PSNR and R while minimum value for MSE should be obtained [30].

$$\text{SNR}=10\log\left[\frac{\sum_{i=1}^{N}(x_d(n))^2}{\sum_{i=1}^{N}(x(n)-x_d(n))^2}\right] \quad (1)$$

$$\text{PSNR}=20\log\left[\frac{\max[x(n)]}{RMSE}\right] \quad (2)$$

$$\text{MSE}=\frac{\sum_{i=1}^{N}(x(n)-x_d(n))^2}{N} \quad (3)$$

$$\text{R}=\frac{cov\,(x(n)-x_d(n))}{\sqrt{var(x(n))\,var(x_d(n))}} \quad (4)$$

*D. Feature Extraction*

Twelve features were used to describe the five segments in the EEG signal. These features were used to discriminate the segments against each other. These were optimally selected using analysis of variance [32] and graphical discrimination.

- Kurtosis: This is a statistical measure of the flatness or peakedness of a signal distribution. The kurtosis of the power spectrum vector of the EEG signal was used as a feature [24].
- Skewness: This is also a statistical measure but it deals with the asymmetry of a signal distribution. As with kurtosis, the skewness of the power spectrum vector of the EEG signal was used [24].
- Hilbert Spectrum Vectors: This is a two-part transform in which the first part is the empirical mode decomposition (EMD) and the second is the Hilbert-Huang Transform (HHT) which outputs a non-normalized joint amplitude-frequency-time distribution [23]. Graphically, the output is a spline curve. Using numerical integration, the area under the spline curve was used as a feature.
- Power Spectrum Vectors: These are derived from the Hamming-windowed Fourier transform of the EEG signal. The power spectrum vectors were decomposed using Singular Value Decomposition (SVD) to represent a single feature [25].
- Root Mean Square (RMS): With reference to the results from [24], the beta/alpha power ratio of the 5 segments are found to be of significance hence, their respective RMS voltages were considered as one of the features.
- Band Power: This is a feature that describes the average power that exists in a signal vector [33].
- Spurious Free Dynamic Range: This is a logarithmic feature, expressed in dB, which computes the power spectrum using a modified periodogram with a Hamming window. The difference from a power spectrum vector is that the mean is subtracted from the input signal before computing the power spectrum. The number of points in the computation of the Discrete Fourier Transform (DFT) is equal to the length of the input signal.
- State Levels: This feature shows the lower and upper estimation of the state levels of a bi-level input vector using a 100-bin histogram whose lower and upper bounds correspond to the minimum and maximum value, respectively, found in the input vector. The histogram is divided into two equally sized regions between the first and last non-zero bin. The feature vectors are represented by the mode of each region.
- Root Sum Squared Value: This feature describes the root-sum-of-squares of an input vector. Since this will output a vector, the mean of the output vector is considered as a feature.
- Delay between Signals: This features estimates the delay between two signals. Having known that the other four segments has a difference with the baseline segment [24], the delay of the baseline segment was computed with reference to each of the four segments.
- Entropy: This feature is a measure of the level of disturbance or uncertainty [34]. With the given relaxed and stimulated states of the EEG signals, the level of how a relaxed EEG signal is disturbed once a musical tone is heard can be determined using entropy calculations. Hence, this was considered as one of the significant features.

*E. Artificial Neural Networks (ANN)*

An artificial neural network consists of a pool of simple processing units ('neurons' or 'cells') which communicate by sending signals to each other over a large number of weighted connections [35]. These processing units receive input from neighbor units or from external sources and use it to compute an output signal which is sent to the other units. Aside from this, weight adjustment is also performed.

Neural systems have three useful types of units: the input units (which receive data from external sources or outside the neural network), the hidden units (whose input and output data remain with the neural network) and the output units (which send data out of the neural network). In other terminologies, units are termed as layers.

In this study, a three-layer feed-forward neural network was used [20]. The function fitting neural network architecture is shown in Fig. 4. The input layer is composed of 12 neurons which correspond to the 12 features of the EEG signals. Each input neuron is connected to the 50 sigmoid neurons that forms the hidden layer. The hidden neurons are connected to the output layer which is composed of 5 linear output neurons that corresponds to BL, s-BL, C, F and G. Systems based on ANN uses neural networks for training to create defining boundaries around data points or between data sets [27]. This algorithm requires training, validation and testing.

The input vector is represented by the features arranged in a 12 x 165 matrix. The input vector is paired with a 5 x 165 target matrix for training. The 165 columns were obtained from the number of segments multiplied by the number of

respondents. The features were divided into 60% training set, 20% validation set and 20% testing set. The data simulation was performed in Matlab.

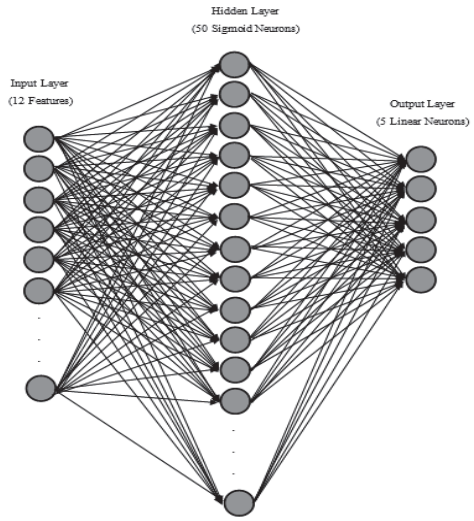


Fig. 4. Function Fitting Neural Network Diagram

The network was trained with scaled conjugate gradient Bayesian Regulation backpropagation: a training function that updates the weight and bias values according to the Levenberg-Marquardt (LM) optimization method [36]. This training algorithm minimizes a combination of squared errors and weights, and determines the correct combination in order to produce a network that generalizes well [37]. Bayesian regulation introduces network weights into the training objective function which is denoted by

$$F(w) = \alpha S_w + \beta S_D \tag{5}$$

where $S_w$ is the sum of the squared network weights and $S_D$ is the sum of the network errors. The variables $\alpha$ and $\beta$ are the objective function parameters. The weights of the network are randomly selected and the distribution of the network weights and training set are considered as Gaussian.

The objective function parameters, $\alpha$ and $\beta$, are defined using the Baye's theorem which basically relates two variables, say A and B, according to their prior and posterior probabilities [38]. The posterior probability of A conditional on B is defined by

$$P(A|B) = \frac{P(B|A)P(A)}{P(B)} \tag{6}$$

where P(B | A) is the prior of B conditional to A, P(A) and P(B) are the non-zero prior probabilities of A and B, respectively. The optimal weight space can be obtained by minimizing the objective function in (5) which is equivalent to maximizing the posterior probability function given by

$$P(\alpha, \beta|D, M) = \frac{P(D|\alpha, \beta, M)\, P(\alpha, \beta|M)}{P(D|M)} \tag{7}$$

where $\alpha$ and $\beta$ are the factors to be optimized, D is the weight distribution, M is the particular neural network architecture, P(D | M) is the normalization factor, P($\alpha$, $\beta$ | M) is the uniform prior density for the regularization parameters and P($D$ | $\alpha$, $\beta$, M) is the likelihood function of D given $\alpha$, $\beta$ and M. This process results to optimum values of $\alpha$ and $\beta$ for a given weight space. The LM phase calculates the Hessian (squared second-order partial derivatives of the objective function) and updates the weights in order to minimize the objective function. If convergence is not met, the algorithm estimates new values for $\alpha$ and $\beta$, and the whole process repeats itself until convergence is reached [39].

## III. Results and Discussion

The selection of mother wavelets for de-noising was defined by the conditions in Section II-C. Among the 'db' wavelets used, 'db1' to 'db10', the wavelets 'db8', 'db9' and 'db10' were found to satisfy the selection criteria across the 5 segments.

The SNR, PSNR and correlation coefficient show an increasing trend while MSE shows a decreasing trend from 'db1' to 'db10'. As a requirement, higher SNR, PSNR and correlation coefficient, and lower MSE indicates better de-noising effect. Table II shows the top 3 maximum values for the SNR, PSNR and R, the minimum values for the MSE and the mother wavelet where they were obtained with respect to the 5 segments. Results show that the conditions were satisfied using wavelets 'db8','db9' and 'db10'.

TABLE II. Segment Parameter Values and Significant Wavelets

| Parameters | Segments | | | | | | | | | |
|---|---|---|---|---|---|---|---|---|---|---|
| | BL | | s-BL | | C | | F | | G | |
| SNR(dB) | 19.48 | *db8* | 17.57 | *db10* | 15.59 | *db10* | 16.49 | *db10* | 15.70 | *db10* |
| | 19.52 | *db9* | 17.61 | *db9* | 15.62 | *db8* | 16.53 | *db8* | 15.80 | *db9* |
| | 19.54 | *db10* | 17.61 | *db8* | 15.65 | *db9* | 16.65 | *db9* | 15.81 | *db8* |
| PSNR (dB) | 52.37 | *db8* | 44.93 | *db7* | 42.97 | *db9* | 43.02 | *db8* | 42.95 | *db10* |
| | 52.42 | *db9* | 44.99 | *db8* | 42.98 | *db5* | 43.03 | *db10* | 43.00 | *db8* |
| | 52.45 | *db10* | 45.14 | *db10* | 43.05 | *db8* | 43.10 | *db9* | 43.09 | *db9* |
| MSE | 0.7675 | *db8* | 1.1956 | *db8* | 1.5136 | *db9* | 1.3072 | *db10* | 1.4160 | *db10* |
| | 0.7592 | *db9* | 1.1903 | *db10* | 1.5129 | *db6* | 1.3005 | *db9* | 1.3936 | *db8* |
| | 0.7556 | *db10* | 1.1847 | *db9* | 1.5079 | *db10* | 1.2828 | *db8* | 1.3895 | *db9* |
| R | 0.9897 | *db8* | 0.9844 | *db10* | 0.9795 | *db9* | 0.9823 | *db10* | 0.9815 | *db10* |
| | 0.9899 | *db9* | 0.9845 | *db8* | 0.9795 | *db6* | 0.9824 | *db9* | 0.9817 | *db8* |
| | 0.9899 | *db10* | 0.9845 | *db9* | 0.9796 | *db10* | 0.9826 | *db8* | 0.9817 | *db9* |

The EEG signals were then de-noised using the 3 identified wavelets. Feature extraction was performed to determine the 12

features as mentioned in Section II-D. These features were used to train the ANN. Five training trials were performed and the average correct classification percentage was obtained. Results are shown in Table III.

TABLE III. CORRECT CLASSIFICATION ACCURACY FOR EACH WAVELET

| Wavelet | Segments | | | | |
|---|---|---|---|---|---|
| | BL | s-BL | C | F | G |
| db8 | 85.45% | 79.39% | 88.48% | 82.42% | **83.03%** |
| db9 | 86.06% | 76.36% | **91.52%** | 83.64% | 81.82% |
| db10 | **89.09%** | **80.00%** | 83.03% | **86.06%** | 80.61% |

High correct classification results ranging from 80% to around 92% were obtained and it is noticeable that the highest classification does not occur only by using a single type of wavelet with respect to each segment. This is possibly due to the form of the wavelet with respect to a given segment [30]. Referring to Fig. 3, 'db8' to 'db10' shows higher resemblance of the EEG waveforms as shown in Fig. 2. For BL, the highest correct classification result was obtained when the EEG signal is de-noised using 'db10'. This is the same with the s-BL and F segments. The C segment has the highest correct classification accuracy when 'db9' was used while the G segment is when 'db8' was used. For s-BL, 'db8' can also be considered as the accuracy is not that significantly far from using 'db10'.

Confusion matrices are used to assess the performance of different classifiers [40], [41]. These matrices provide information that leads to measuring the sensitivity, specificity, precision, accuracy and F-score of the classifier. Precision tells how many of the positively classified were relevant, sensitivity / recall tells how good a test is in detecting the positives, and specificity tells how good a test is in avoiding false detections. The F-score is the harmonic mean of precision and sensitivity. Table IV shows the confusion matrices for the ANN when 'db8', 'db9' and 'db10' was used.

TABLE IV. CONFUSION MATRICES

| | | Target Class | | | | |
|---|---|---|---|---|---|---|
| | | BL | s-BL | C | F | G |
| Output Class | BL | 32 | 0 | 0 | 0 | 0 |
| | s-BL | 2 | 26 | 1 | 1 | 0 |
| | C | 0 | 1 | 28 | 2 | 0 |
| | F | 2 | 1 | 1 | 25 | 1 |
| | G | 0 | 0 | 1 | 1 | 23 |

a. Using db8

| | | Target Class | | | | |
|---|---|---|---|---|---|---|
| | | BL | s-BL | C | F | G |
| Output Class | BL | 29 | 0 | 0 | 1 | 0 |
| | s-BL | 1 | 28 | 0 | 2 | 2 |
| | C | 1 | 1 | 26 | 2 | 0 |
| | F | 1 | 0 | 0 | 30 | 0 |
| | G | 1 | 1 | 2 | 1 | 27 |

b. Using db9

| | | Target Class | | | | |
|---|---|---|---|---|---|---|
| | | BL | s-BL | C | F | G |
| Output Class | BL | 33 | 0 | 0 | 0 | 0 |
| | s-BL | 0 | 28 | 2 | 0 | 1 |
| | C | 1 | 1 | 29 | 2 | 0 |
| | F | 1 | 3 | 2 | 26 | 0 |
| | G | 1 | 2 | 4 | 1 | 23 |

c. Using db10

By taking into account the instances between the target and output classes, Table V was derived. Results show high precision, sensitivity, specificity, accuracy and F-score. The highest accuracy and F-score for the BL segment was obtained using 'db10'. For the s-BL and G segments, 'db8' exhibits the highest accuracy. For the F segment, 'db9' shows the highest accuracy. 'db9' and 'db8' shows the highest accuracy and F-score for the C segment, respectively.

TABLE V. PRECISION, SENSITIVITY, SPECIFICITY, ACCURACY AND F-SCORE TABLE

| Segment | Precision | Sensitivity | Specificity | Accuracy | F-score |
|---|---|---|---|---|---|
| BL | 88.89 | 100.00 | 96.23 | 97.10 | 94.12 |
| s-BL | 92.86 | 86.67 | 98.18 | 95.71 | 89.66 |
| C | 90.32 | 90.32 | 97.25 | 95.71 | 90.32 |
| F | 86.21 | 83.33 | 96.46 | 93.71 | 84.75 |
| G | 95.83 | 92.00 | 99.11 | 97.81 | 93.88 |

a. Using db8

| Segment | Precision | Sensitivity | Specificity | Accuracy | F-score |
|---|---|---|---|---|---|
| BL | 87.88 | 96.67 | 96.52 | 96.55 | 92.06 |
| s-BL | 93.33 | 84.85 | 98.25 | 95.24 | 88.89 |
| C | 92.86 | 86.67 | 98.28 | 95.89 | 89.66 |
| F | 83.33 | 96.77 | 94.83 | 95.24 | 89.55 |
| G | 93.10 | 84.38 | 98.26 | 95.24 | 88.52 |

b. Using db9

| Segment | Precision | Sensitivity | Specificity | Accuracy | F-score |
|---|---|---|---|---|---|
| BL | 91.67 | 100.00 | 97.25 | 97.89 | 95.65 |
| s-BL | 82.35 | 90.32 | 94.87 | 93.92 | 86.15 |
| C | 78.38 | 87.88 | 93.22 | 92.05 | 82.86 |
| F | 89.66 | 81.25 | 97.41 | 93.92 | 85.25 |
| G | 95.83 | 74.19 | 99.15 | 93.92 | 83.64 |

c. Using db10

## IV. CONCLUSION AND FUTURE DIRECTIVES

Musical tone stimulated EEG signals were analyzed and classified in this study. Wavelet-based de-noising with thresholding was used using different Daubechies wavelets ('db1' to 'db10'). Since wavelet transform performs a correlation analysis, the output is expected to be maximal when the input signal most resembles the mother wavelet.

The EEG signals were segmented into Baseline, secondary baseline, C, F and G tones and were classified accordingly using ANN. Among the ten wavelets used for de-noising, it was found out that 'db8','db9' and 'db10' were able to satisfy the conditions set which are defined by high SNR, PSNR and R, and low MSE.

The highest correct classification accuracy was not attained using a single type of wavelet. As shown in Table III, each segment may be de-noised using different wavelets in order to give high classification accuracies. Each segment has different characteristics which can be addressed not only by a single wavelet. The ANN was assessed using confusion matrices and results show high precision, sensitivity, specificity, accuracy and F-score percentages.

Other wavelets (higher db wavelets, Coiflets, Biorthogonal, Reverse Biorthogonal, Discrete Meyer and Symlets) and de-noising thresholding techniques ('rigrsure', 'heursure', 'minimaxi') can be explored as they can be used to provide

higher classification accuracies. In addition, how each (or combinations) of the 12 features impact classification accuracies could be explored using other classifiers like support vector machines and k-means algorithm.

## REFERENCES


[1] M. G. Quiñones, A. Kassabian, and E. Boschi, *Ubiquitous musics: The everyday sounds that we don't always notice*. Farnham: Ashgate Publishing, Ltd., 2013.

[2] H. T. Ocbagabir, K. a I. Aboalayon, and M. Faezipour, "Efficient EEG analysis for seizure monitoring in epileptic patients," *9th Annu. Conf. Long Isl. Syst. Appl. Technol. LISAT 2013*, 2013.

[3] N. V. T. Shanbao Tong, *Quantative EEG Analysis Methods and Clinical Applications*. 2009.

[4] M. a. Sovierzoski, F. I. M. Argoud, and F. M. De Azevedo, "Identifying eye blinks in EEG signal analysis," *5th Int. Conf. Inf. Technol. Appl. Biomed. ITAB 2008 conjunction with 2nd Int. Symp. Summer Sch. Biomed. Heal. Eng. IS3BHE 2008*, no. 2, pp. 406–409, 2008.

[5] M. Esmaeili, M. H. Jabalameli, and Z. Moghadam, "A New Scheme of EEG Signals Processing in Brain-Computer Interface Systems," *2007 IEEE Int. Conf. Granul. Comput. (GRC 2007)*, pp. 522–527, 2007.

[6] L. Z. L. Zou, X. W. X. Wang, G. S. G. Shi, and Z. M. Z. Ma, "EEG feature extraction and pattern classification based on motor imagery in brain-computer interface," *Cogn. Informatics (ICCI), 2010 9th IEEE Int. Conf.*, 2010.

[7] S. M. Park and K. B. Sim, "A study on the analysis of auditory cortex active status by music genre: Drawing on EEG," *Proc. - 2011 8th Int. Conf. Fuzzy Syst. Knowl. Discov. FSKD 2011*, vol. 3, pp. 1916–1919, 2011.

[8] Q. Dong, Y. Li, B. Hu, Q. Liu, X. Li, and L. Liu, "A solution on ubiquitous EEG-based biofeedback music therapy," *ICPCA10 - 5th Int. Conf. Pervasive Comput. Appl.*, pp. 32–37, 2010.

[9] Y. P. Lin, T. P. Jung, and J. H. Chen, "EEG dynamics during music appreciation," *Proc. 31st Annu. Int. Conf. IEEE Eng. Med. Biol. Soc. Eng. Futur. Biomed. EMBC 2009*, pp. 5316–5319, 2009.

[10] S. K. Hadjidimitriou and L. J. Hadjileontiadis, "Toward an EEG-based recognition of music liking using time-frequency analysis," *IEEE Trans. Biomed. Eng.*, vol. 59, no. 12, pp. 3498–3510, 2012.

[11] Y. Morita, H. H. Huang, and K. Kawagoe, "Towards Music Information Retrieval driven by EEG signals: Architecture and preliminary experiments," *2013 IEEE/ACIS 12th Int. Conf. Comput. Inf. Sci. ICIS 2013 - Proc.*, pp. 213–217, 2013.

[12] H. Lu, M. Wang, and H. Yu, "EEG model and location in brain when enjoying music.," *Conf. Proc. IEEE Eng. Med. Biol. Soc.*, vol. 3, pp. 2695–2698, 2005.

[13] S. Stober and J. Thompson, "Music Imagery Information Retrieval: Bringing the Song on Your Mind back to Your Ears," *13th Int. Conf. Music Inf. Retr. -- Late-Breaking Demo Pap.*, 2012.

[14] M. Mamun, M. Al-Kadi, and M. Marufuzzaman, "Effectiveness of wavelet denoising on electroencephalogram signals," *J. Appl. Res. Technol.*, vol. 11, no. 1, pp. 156–160, 2013.

[15] M. I. Al-Kadi, M. B. I. Reaz, and M. A. Mohd Ali, "Compatibility of mother wavelet functions with the electroencephalographic signal," in *2012 IEEE-EMBS Conference on Biomedical Engineering and Sciences, IECBES 2012*, 2012, no. December, pp. 113–117.

[16] P. Kumari and A. Vaish, "Brainwave based user identification system: A pilot study in robotics environment," *Rob. Auton. Syst.*, vol. 65, pp. 15–23, 2015.

[17] P. Kumari and A. Vaish, "Information-Theoretic Measures on Intrinsic Mode Function for the Individual Identification Using EEG Sensors," *IEEE Sens. J.*, vol. 15, no. 9, pp. 4950–4960, 2015.

[18] P. Kumari and A. Vaish, "Feature-level fusion of mental task's brain signal for an efficient identification system," *Neural Comput. Appl.*, vol. 27, no. 3, pp. 659–669, 2016.

[19] V. B. Semwal, M. Raj, and G. C. Nandi, "Biometric gait identification based on a multilayer perceptron," *Robot. Auton. Syst.*, vol. 65, pp. 65–75, 2015.

[20] V. B. Semwal, K. Mondal, and G. C. Nandi, "Robust and accurate feature selection for humanoid push recovery and classification: deep learning approach," *Neural Comput. Appl.*, pp. 1–10, 2015.

[21] T. Gagnon, S. Larouche, and R. Lefebvre, "A neural network approach for preclassification in musical chords recognition," *Thrity-Seventh Asilomar Conf. Signals, Syst. Comput. 2003*, vol. 2, pp. 2106–2109, 2003.

[22] A. Subasi and E. Erçelebi, "Classification of EEG signals using neural network and logistic regression," *Comput. Methods Programs Biomed.*, vol. 78, no. 2, pp. 87–99, 2005.

[23] J. Kim, B. Şen, and et al, "Sleep stage classification based on EEG hilbert-huang transform," *Conf. Proc. ... Annu. Int. Conf. IEEE Eng. Med. Biol. Soc. IEEE Eng. Med. Biol. Soc. Annu. Conf.*, vol. 2014, no. 3, pp. 1–6, 2014.

[24] R. F. Navea and E. Dadios, "Beta/Alpha power ratio and alpha asymmetry characterization of EEG signals due to musical tone stimulation," in *Project Einstein 2015*, 2015.

[25] R. F. Navea and E. Dadios, "Classification of tone stimulated EEG signals using independent components and power spectrum vectors," in *2015 International Conference on Humanoid, Nanotechnology, Information Technology,Communication and Control, Environment and Management (HNICEM)*, 2015, December, pp. 1–5.

[26] T. Collura, *Technical Foundations of Neurofeedback*. Abingdon: Routledge, 2014.

[27] S. Dua and P. Chowriappa, *Data Mining for Bioinformatics Applications*. Boca Raton: CRC Press, 2015.

[28] S. Sanei and J. A. Chambers, *EEG Signal Processing*. West Sussex: John Wiley & Sons Ltd, 2007.

[29] S. Garg and R. Narvey, "Denoising and Feature Extraction of EEg Signal Using Wavelet Transform," *Int. J. Eng. Sci. Technol.*, vol. 5, no. 6, pp. 1249–1253, 2013.

[30] N. K. Al-Qazzaz, S. Ali, S. A. Ahmad, M. S. Islam, and M. I. Ariff, "Selection of mother wavelets thresholding methods in denoising multi-channel EEG signals during working memory task," *IECBES 2014, Conf. Proc. - 2014 IEEE Conf. Biomed. Eng. Sci. "Miri, Where Eng. Med. Biol. Humanit. Meet,"* December, pp. 214–219, 2015.

[31] "Introduction to Wavelet Families." [Online]. Available: http://www.mathworks.com/help/wavelet/gs/introduction-to-the-wavelet-families.html.

[32] J. Singha and R. H. Laskar, "Hand gesture recognition using two-level speed normalization, feature selection and classifier fusion," *Multimdia Syst.*, pp. 1–16, 2016.

[33] M. S. A. M. Ali, M. N. Taib, N. M. Tahir, and A. H. Jahidin, "EEG spectral centroid amplitude and band power features: A correlation analysis," *Proc. - 2014 5th IEEE Control Syst. Grad. Res. Colloquium, ICSGRC 2014*, pp. 223–226, 2014.

[34] R. F. Navea and E. Dadios, "Design and Implementation of a Cascaded Adaptive Neuro-Fuzzy Inference System for Cognitive and Emotional Stress Level Assessment based on Electroencephalograms and Self-Reports," in *HNICEM*, 2014, November 2014

[35] B. Krose and P. van der Smagt, *An Introduction to Neural Networks*, The University of Amsterdam, November 1996.

[36] L. B. Nguyen, A. V. Nguyen, S. H. Ling, and H. T. Nguyen, "Combining genetic algorithm and Levenberg-Marquardt algorithm in training neural network for hypoglycemia detection using EEG signals," *Proc. Annu. Int. Conf. IEEE Eng. Med. Biol. Soc. EMBS*, pp. 5386–5389, 2013.

[37] X. Pan, B. Lee, and C. Zhang, "A comparison of neural network backpropagation algorithms for electricity load forecasting," in *IEEE International Workshop on Intelligent Energy Systems (IWIES)*, pp. 22–27, 2013

[38] G. Li and J. Shi, "Applications of Bayesian methods in wind energy conversion systems," *Renew. Energy*, vol. 43, pp. 1–8, 2012.

[39] Z. Yue, Z. Songzheng, and L. Tianshi, "Bayesian regularization BP Neural Network model for predicting oil-gas drilling cost," in *International Conference onBusiness Management and Electronic Information (BMEI)*, 2011.

[40] M. Pal and S. Bandyopadhyay, "Many-objective feature selection for motor imagery EEG signals using differential evolution and support vector machine," in *International Conference on Microelectronics, Computing and Communications*, 2016.

[41] S. A. M. Aris, A. H. Jahidin, and M. N. Taib, "Performance measure of the multi-class classification for the EEG calmness categorization study," in *International Conference on BioSignal Analysis, Processing and Systems*, 2015.